Nigerian Journal of Physics (NJP)

ISSN: 1595-0611

Volume 32(1), March 2023

Optimisation of PCBM on Al_2O_3 Electron Transport Layer for Improved Performance of Perovskite Solar Cells Using SCAPS 1D

[1,2]Goje, A. A., [2]Ludin, N. A., *[1]Sheriff, M. A., [1]Zanna, M. W. and [3]Isah, M.

[1]Department of Science Laboratory Technology, Federal Polytechnic Damaturu, P.M.B. 1006, Yobe State, Nigeria
[2]1Solar Energy Research Institute (SERI), Universiti Kebangsaan Malaysia, 43600, Bangi, Selangor Darul Ehsan, Malaysia
[3]Department of Physics, Kaduna State University, PMB 2339, Tafawa Balewa Way. Kaduna, Nigeria.

*Corresponding author's email: muhiddin002@gmaiil.com

ABSTRACT

Despite strides in perovskite solar cell efficiency, hurdles hamper industrialization and commercialization. Stability issues, limited electron extraction, and high charge recombination rates cause rapid degradation. Researchers target perovskite material enhancement, using SCAPS software to optimize the electron transport layer (ETL) and introduce Aluminum oxide (Al_2O). This aims to boost electron extraction, cut recombination losses, and enhance overall stability. Common ETLs like [6,6]-phenyl C61 butyric acid methyl ester/Aluminum oxide (PCBM/Al_2O_3) are standard, aiding electron transportation from the perovskite to the electrode. Our study focuses on an n-i-p planar lead-free heterostructure PSC setup, comprising Glass/Fluorine-doped Tin Oxide (FTO), Al_2O_3/PCBM (ETL), methyl ammonium lead iodide ($CH_3NH_3PbI_3$) as the absorber, Spiro-OMeTAD as the Hole Transport Layer (HTL), and silver (Ag) as the electrode. Optimization efforts included a 100 nm absorber layer and 300 K temperature, considering ETL thickness and defect density. The PSC's defect density was inversely linked to its absorption coefficient (alpha). Using solely Al_2O_3 layer achieved a power conversion efficiency (PCE) of 10.87%, a current density (J_{sc}) of 31.62 mA/cm^2, an open circuit voltage (V_{oc}) of 0.551V, and a fill factor (FF) of 61.39%. In contrast, employing optimized Al_2O_3/PCBM ETL led to improved performance, yielding a PCE of 20.61%, a J_{sc} of 37.23 mA/cm^2, a V_{oc} of 0.569 V, and an FF of 68.11%. Additionally, an inverse relationship emerged between FF, ETL thickness, and 300 K temperature.

Keywords:
Perovskite solar cell, Al_2O_3/PCBM ETL, SCAPS simulation software.

INTRODUCTION

The performance of photovoltaic (PV) devices depends on the electron transport layer (ETL) in the solar cell (Wang *et al*., 2021) (Goje *et al.*, 2023). A vital function of the ETL is facilitating the efficient transport of electrons generated by light absorption into the electrodes (Bouhjar et al., 2020). There have been numerous efforts to optimise the ETL in PV devices. In particular, the combination of poly(3-hexylthiophene) (P3HT) and phenyl-C61-butyric acid methyl ester (PCBM) has become a popular choice for the ETL due to its high electron mobility and ease of processing. The study addresses challenges in inverted perovskite solar cells (PSCs) using PCBM as the ETL, which leads to lower efficiency due to issues like low electron mobility and nonradiative recombination. The researchers introduced a strategy by combining PCBM with conjugated n-type polymeric materials to create a homogeneous bulk-mixed (HBM) film with enhanced electron mobility. They reduced nonradiative recombination at the perovskite/HBM interface. This approach resulted in inverted PSCs with efficiency exceeding 20.6% and improved stability, with HBM-based devices retaining 80% of their initial efficiency after 45 days of ageing, compared to 48% for control devices (Yang et al., 2019). This study focused on optimising the performance of PSCs by simulating different metal back contacts (Silver (Ag), Chromium (Cr), Copper (Cu), Gold (Au), Nickle (Ni), and Platinum (Pt)) with and without a hole transport material (HTM). The research found that the metal contact's work function significantly influenced the PSCs' photovoltaic performance, with Pt being the best choice for both HTM and HTM-free configurations. The optimised devices achieved substantial enhancements, with a power conversion efficiency (PCE) of 27.423%

and 26.767% for HTM-free and HTM-based PSCs, respectively, representing approximately a 1.05 to 1.07-fold improvement in PCE and current density (J_{sc}) over the unoptimised cell (Danladi, Gyuk, et al., 2023). The choice of material (Brown *et al.,* 2021), the thickness of the layer (Bag *et al*., 2020), and the processing conditions adversely affect the overall performance of a device, where she will focus on optimising a single or double layer ETL. In recent years, several studies have explored the impact of these factors on the performance of PV devices. The materials used in these studies include PCBM, Al_2O_3, and $MAIPbI_3$, among others.

One standard method for optimising the PCBM on Al_2O_3 ETL is to control the thickness of the single layer, keeping the other layer constant. Erazo ET AL. (2021) explored an alternative and cost-effective approach for enhancing the PCE of PSCs. Instead of using the single ETL, they employ a double ETL to deposit an organic-inorganic bilayer of PEDOT: PSS-Cl-Al_2O_3, followed by annealing. This material was found to improve solar cell performance on Al_2O_3.

EETL-only devices, resulting in an increase in PCE from 12.1% to 14.3% (Erazo *et al*., 2021). A report utilises the SCAPS-1D) to investigate the performance of mixed halide PSCs. Mandadapu ET AL. (2022) employed PCBM as ETL and explored the various parameters, including absorber layer thickness, defect density, and operating temperature, to optimise the cell's PCE. Through simulation, the study predicts PCEs exceeding 26%, demonstrating the potential for high-performance mixed halide PSCs, and validates its findings through experimental comparison (Mandadapu *et al*., 2022). The highest PCE was achieved with an Al_2O_3 layer thickness of 50 nm, attributed to improved electron transport through the ETL. Another critical factor in optimising the PCBM/ Al_2O_3 ETL is the choice of material. In a study by Lee ET AL. (2021), the impact of the type of Al_2O_3 on the performance of PV devices was investigated (Lee et al., 2021). They found that using Al_2O_3 nanorods instead of Al_2O_3 nanoparticles significantly improved the PCE of the PV device. The improved performance was attributed to the increased surface area of the Al_2O_3 nanorods, which facilitated the efficient transport of electrons.

The processing conditions used to fabricate the PCBM/ Al_2O_3 ETL can also significantly impact its performance. Yang *et al.* (2019) explored the effect of annealing temperature on the performance of PV devices. They found in their study that annealing at a temperature of 500°C significantly improved the PCE of the PV device compared to annealing at a temperature of 300°C (Yang *et al.,* 2019). The improved performance was attributed to the increased crystallinity of the P3HT and PCBM in the ETL after annealing at 500°C. The ETL plays a crucial role in determining the performance and stability of PSCs. In recent years, PSCs have gained significant attention as a promising alternative to traditional silicon-based solar cells due to their high PCE and low cost. However, the stability of PSCs remains a significant challenge, with degradation occurring primarily at the ETL interface.

One commonly used ETL in PSCs combines PCBM and Aluminium Oxide (Al_2O_3). The PCBM has shown promise as an ETL due to its ability to enhance the stability and PCE of PSCs, where it achieved a PCE of 20.6%; the results showed that a thicker PCBM layer with a smooth surface and a larger grain size improved performance and stability in PSCs (Yang *et al.,* 2019). To optimise the PCBM/ Al_2O_3 ETL in PSCs, various factors must be considered, such as the thickness and surface roughness of the Al_2O_3 layer and the coverage and grain size of the PCBM layer. Simulations play a crucial role in optimising the ETL, as they allow for predicting the performance and stability of PSCs under various conditions. One widely used simulation software for optimising the ETL in PSCs is Simulation of Charged Particles and PV Systems (SCAPS) 1D, which is software designed for simulating the electronic and optical properties of PSC and other solar cells, aiding in the analysis and optimisation of their performance in various electronic device (Burgelman *et al.,* 2021). Recently, investigated Tin-based PSCs for their eco-friendly properties, using numerical modelling and SCAPS-1D software to analyse their performance. The study achieved a substantial PSC performance through optimisation, suggesting the potential for cost-effective, eco-friendly, and highly efficient PSCs that compete with state-of-the-art technology (Danladi, Kashif *et al.,* 2023). The software can simulate the transport of electrons in PSCs and has been used to optimise the PCBM/Al_2O_3 ETL (Khalid Hossain *et al.,* 2022). Reyes *et al.* (2021) employed SCAPS 1D to optimise the ETL for improved performance and stability in PSCs (Reyes *et al.,* 2021). Also, Eli ET AL. (2021), in their work, consider simulating an efficient lead-free PSC with a structure made up of layers of FTO, TiO_2, $MASnI_3$, CZTS, and Au. The simulation investigates acceptor concentration, defect density, temperature, band gap, and absorber thickness. According to the results, the top-performing arrangement had a J_{sc} of 31.66 mA/cm^2, V_{oc} of 0.96 V, FF of 67%, and PCE of 20.28%, making it appropriate for solar energy harvesting applications (Reyes et al., 2021). Another study by Mandadapu ET AL. (2017) used a lead-based PSC model with a flexible architecture. It optimised various parameters, such as absorber layer thickness and electron transport and hole transport materials doping concentrations. By doing so, they significantly improved PCE, with a maximum PCE of 31.77%, representing a 4-5% enhancement over previous models (Mandadapu, 2017). Optimising the PCBM on Al_2O_3 ETL in PSCs is crucial for improved

performance and stability. SCAPS 1D simulation software is a valuable tool for optimising the ETL, as it predicts the performance and stability of PSCs under various conditions. The ETL can be optimised by considering factors such as the thickness and roughness of the PCBM layer. This work is aimed at optimizing the PCBM on Al_2O_3 ETL for enhanced Performance of perovskite solar cells employing SCAPS 1D software.

Device structures

The $MAPbI_3$ absorption layer is presumed to be placed between the ETL/HTL layers in the device structure, as depicted in Figure 1 below. To enhance the PCE, the PCBM ETL on a double ETL layers perovskite is varied extensively. Consequently, a PV device simulation was conducted for a PSC based on PCBM on Al_2O_3 ETLs using an FTO/Al_2O_3/PCBM/$MAPbI_3$/Spiro-OMeTAD/Ag planar heterojunction in an n-i-p mode setup. Silver (Ag) was chosen as the metal rear contact, possessing a work function of 4.3 eV. Light incidences were considered across Glass/FTO layers, assumed to have a thickness of 200 nm with a transmissivity of 89% and a surface resistance of 15 ohm/sq. The simulation utilized the solar cell capacitance simulator under the 1 Sun spectrum of the software. The modelling process considered the thicknesses of the PCBM deposited on the Al_2O_3 ETL. PCBM and Al_2O_3 served as ETLs in the PSC device, with various thicknesses analyzed to determine the device's performance.

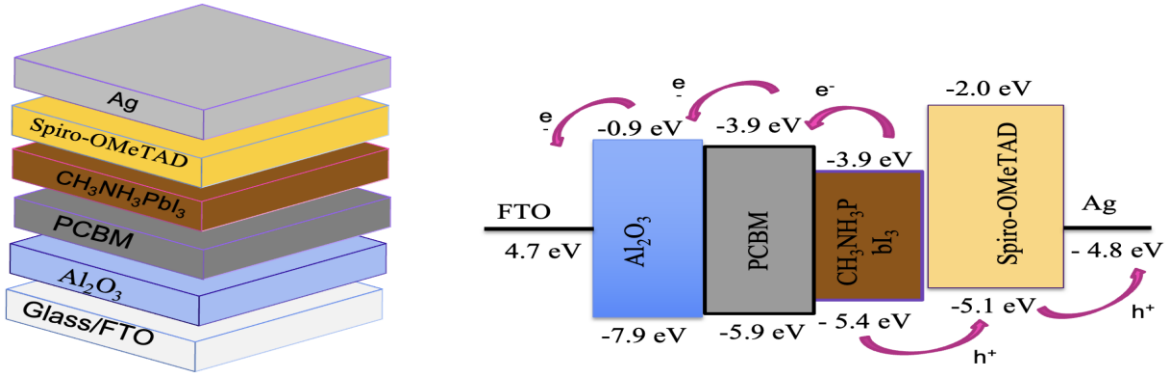

Figure 1: (a) The architecture of the PSC devices simulated (b) the energy band diagram (Yang *et al.*,2019).

MATERIALS AND METHODS

Simulation has become an indispensable resource for researchers as it offers in-depth comprehension and aids in experimental optimization. It significantly contributes to the study of optical and electrical material parameters, enabling predictions about device behaviour (Katubi *et al.*, 2023). The Numerical Simulation SCAPS-1D is a pivotal numerical modelling tool for analyzing semiconductor structures' properties. It operates by solving fundamental semiconductor equations, namely the Poisson equation and the electron and hole continuity equations. In their bulk form, these equations are represented by Constitutive Equations (1) – (5) (Reyes *et al.*, 2021). The Poisson equation delineates the relationship between the electric field of a p-n junction (E) and the space charge density (ρ).

$$\frac{\partial^2\psi}{\partial^2 x} = -\frac{\partial E}{\partial x} = -\frac{\rho}{\varepsilon_S} = -\frac{q}{\varepsilon_S}\left[p - n + N_D^{+}(x) - N_A^{-}(x) \pm N_{def}(x)\right] \quad (1)$$

Where ψ is the electrostatic potential, q is the elementary charge, ε_S is the static relative permittivity, p, n are the electron, and hole density, N_D^{+}, N_A^{-} are the densities of ionized donors and acceptors and N_{def} is the defect density (acceptor or donor).

The electron and hole continuity equations in steady state are

$$\frac{\partial j_n}{\partial x} + G - U_n(n,p) = 0, \quad (2)$$

$$\frac{-\partial j_p}{\partial x} + G - U_p(n,p) = 0, \quad (3)$$

Where $j_{n(p)}$ is the electron and hole current densities, $U_{n(p)}$ is the recombination rates and G is the electron–hole generation rate.

The electron and hole current density are expressed as:

$$j_n = qn\mu_n E + qD_n\frac{\partial n}{\partial x}, \quad (4)$$

$$j_p = qn\mu_p - qD_p\frac{\partial p}{\partial x}, \quad (5)$$

Where q is the elementary charge, $\mu_{n(p)}$ is the electron and hole mobility and $n(p)$ D is the diffusion coefficient of electrons and holes. $n(p)$

Regarding to process simulation, the diagram in Figure 2 shown the steps to build regarding to process simulation of the proposal device.

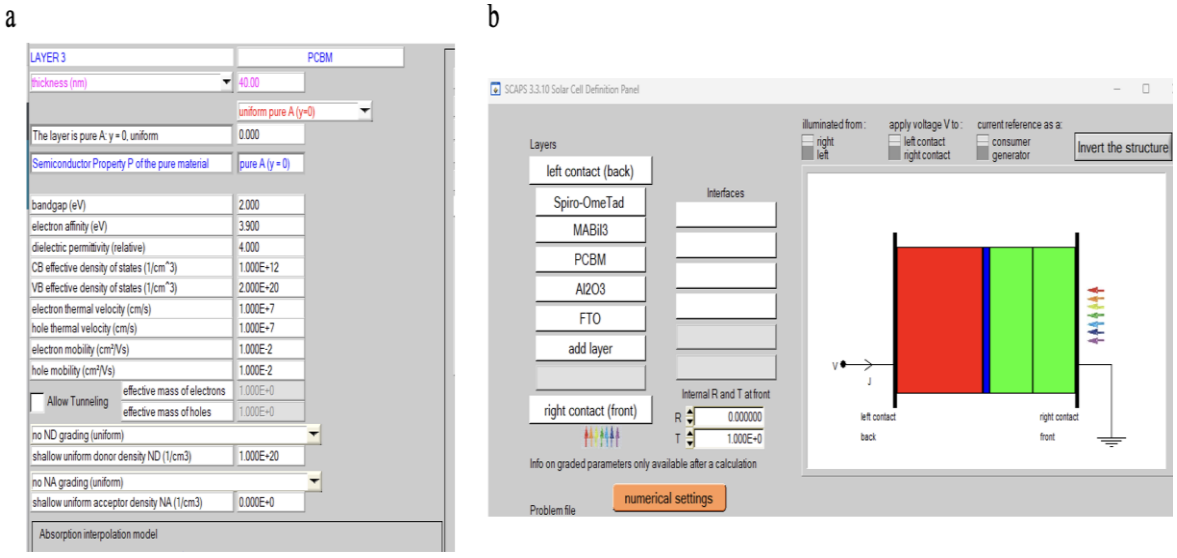

Figure 2: The SCAPS 1D simulation procedure (a) inputting parameters (b) setting working conditions

Optimising Thickness

Layer thickness simulations were conducted using simulation software, predating SCAPS 3.3.00, released in 2014, wherein layer thickness input values were measured in micrometres (µm), ranging from 1 nanometer (nm) (0.001 µm) to 10 centimetres (10^5 µm), displayed with three decimal digits. Inputs below 1 nm were automatically set to 0.001 µm (equivalent to 10^{-5} nm), causing inconvenience; for instance, inputting d = 0.0025 µm (2.5 nm) led the software to calculate 2.5 nm but display it as 0.002 m (2 nm). The acceptable input range for thickness is 0.01 nm (10^{-5} µm), and 1 m equals 10^6 µm. Users had the flexibility to choose various units for thickness display—Angstrom (Å), nanometers (nm), micrometres (µm), millimetres (mm), and centimetres (cm)—while being restricted to three decimal digits. Opting for a measurement other than the standard micrometre resulted in the value and unit being presented in magenta (Burgelman et al., 2021). For example, setting the display unit to µm required inputting 0.00245, displaying the result rounded to three digits, or 0.002 µm. Conversely, switching the display unit to nm showcased the value as 2.45 nm (refer to Figure 3). During newer data import from a file, the software presented thickness in nm if d was ≥ 10 nm, nm if d was ≥ 1000 m, and mm if d > 1 mm. During our experimentation, this display unit adaptation was utilized to modify the ETL layer thickness within a double ETL perovskite device.

Figure 3: The representation of layer thickness with an input of d = 0.00245 µm and meters (m) as the display unit is shown in black (a), while the display unit is switched to nanometers (nm), showcased in pink colour (b) (Burgelman *et al.*,2021.).

RESULT AND DISCUSSION

Measurements from structural profilometry and experimental absorption spectra were utilized to ascertain a Spiro-OMeTAD (HTL) thickness of 350 nm (Haidari, 2019). Additionally, the simulation incorporated the experimental PCBM thickness while setting the Al_2O_3 (ETL) thickness at 30 nm (Lin *et al.*, 2017) (Slami & Merad, 2022). Other pertinent variables, including electron affinity, dielectric permittivity, CB effective density of states, VB effective density of states, charge mobility, thermal velocities, doping densities, and defect densities, were drawn from literature sources (Azri *et al.*, 2019) (Slami & Belkaid, 2020a), (Kuang *et al.*, 2018) (Tan *et al.*, 2016), (Katubi *et al.*, 2023). Figure 4 illustrates the V_{oc} against J_{sc} for different PCBM layer thicknesses on Al_2O_3, determined through simulation software and plotted using Origin 2021 software. The investigation revealed that the ETL thickness significantly impacts device performance. In PSCs, ETL thickness is pivotal in optimizing light absorption, charge transport, and interface properties, directly influencing device efficiency. Precise adjustment of ETL thickness is crucial to strike an optimal balance for efficient energy conversion in PSCs. Notably, J_{sc} and V_{oc} exhibited their highest values at a 40 nm thickness, directly correlating with superior device performance. Table I shows the materials properties of various layers simulated.

Table 1: Materials properties of various layers simulated

Parameters	FTO	Al_2O_3	PCBM	$CH_3NH_3PbI_3$	Spiro-OMeTAD
Thickness (nm)	200	30	Varied	200	350
Band gap (eV)	3.65	1.80	2.00	1.3	2.88
Electron affinity (eV)	4.80	3.90	3.90	4.17	2.05
Dielectric permittivity	8.90	4.50	4.00	6.50	3.00
CB effective density of states ($1/cm^3$)	5.2×10^{18}	1×10^{13}	1×10^{12}	1×10^{18}	2.2×10^{18}
VB effective density of states ($1/cm^3$)	1.0×10^{18}	2×10^{18}	2×10^{20}	1×10^{19}	1.8×10^{19}
Electron thermal velocity (cm/s)	1.0×10^{8}	1×10^{7}	1×10^{7}	1×10^{7}	1×10^{7}
Hole thermal velocity (cm/s)	1.0×10^{8}	1×10^{7}	1×10^{7}	1×10^{7}	1×10^{7}
Electron mobility (cm^2/ V.s)	1.0×10^{12}	1×10^{-2}	1×10^{-2}	1.6	2.0×10^{-4}
Hole mobility (cm^2/ V.s)	1.0×10^{12}	1×10^{-2}	1×10^{-2}	1.6	2.0×10^{-4}
Shallow uniform donor density N_D ($1/cm^3$)	1.0×10^{12}	1×10^{20}	1×10^{20}	0	0
Shallow uniform acceptor density N_A ($1/cm^3$)	0	0	0	3.2×10^{13}	2.0×10^{19}
Defect density Nt ($1/cm^3$)	1×10^{14}	1×10^{14}	1×10^{14}	1.0×10^{14}	1.0×10^{15}

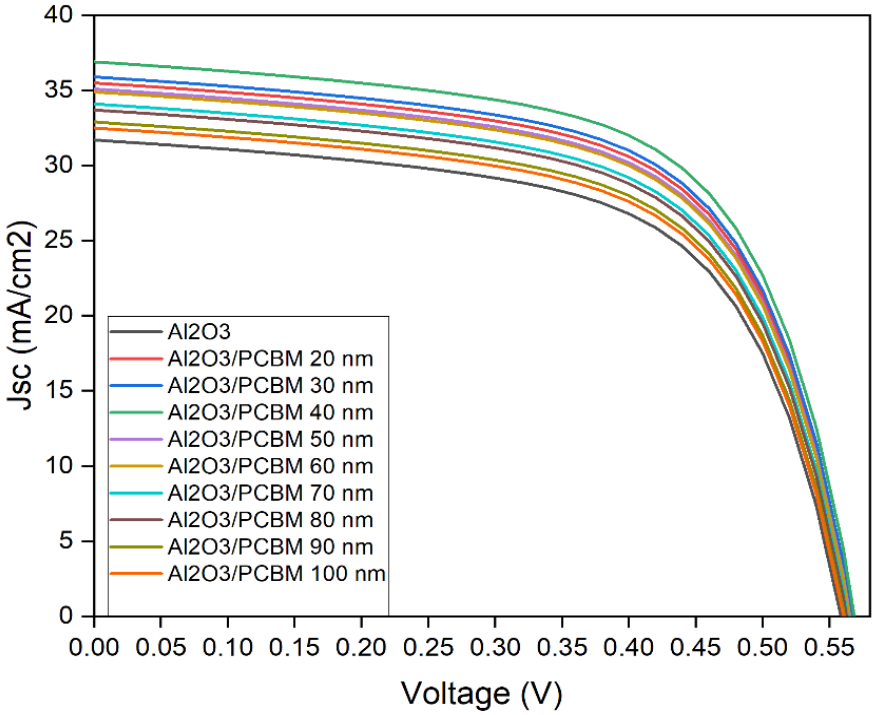

Figure 4: V_{oc} Vs. J_{sc} at different thicknesses of the Al_2O_3 only device and PCBM ELT on Al_2O_3.

The software facilitated numerical simulation and analysis of efficiency, particularly exploring the impact of thickness on the FF in the design involving PCBM on Al_2O_3 ETL. This solar cell configuration comprises FTO/Al_2O_3/PCBM/$CH_3NH_3PbI_3$/Spiro-OMeTAD/Ag. Notably, the ETL layer thickness is crucial in determining performance outcomes. Results indicate several influencing factors, including ETL thickness, FF, and temperature adjustments, to enhance the PCE of $MAPbI_3$-based PSCs. Among the varied designs, the solar cell exhibiting the highest PCE noted at a 40 nm thickness (highlighted in Figure 4 and Table 2), showcased distinct performance metrics. Specifically, the configuration with an Al_2O_3-only layer achieved a PCE of 10.87%, a J_{sc} of 31.62 mA/cm^2, a V_{oc} of 0.551 V, and an FF of 61.39%. In contrast, utilizing an Al_2O_3/PCBM ETL led to improved performance, yielding a PCE of 20.61%, a J_{sc} of 37.23 mA/cm^2, a V_{oc} of 0.569 V, and an FF of 68.11%.

Table 2: Various FF, V_{oc}, J_{sc}, and PCE of the simulated PCS PCBM on Al_2O_3 ELT

Thickness (nm)	Voltage (V)	J_{sc} (mA/cm^2)	FF (%)	PCE (%)
Al_2O_3 (30 nm)	0.551	31.62	61.39	10.87
20	0.564	35.43	63.23	18.04
30	0.561	35.92	64.34	18.52
40	0.569	37.23	68.11	20.61
50	0.559	35.24	63.98	18.00
60	0.554	34.85	63.22	17.43
70	0.552	34.17	62.76	16.91
80	0.551	33.58	62.23	16.44
90	0.547	32.92	62.34	16.03
100	0.541	32.31	61.45	15.34

Table 2 provides information about a material's thickness (nm) and its corresponding PCE (%). The data suggests that there is a trend in the PCE as the thickness of the material varies. The highest efficiency is observed at a thickness of 40 nm, which is 20.61%. However, the efficiency drops for both lower and higher thickness values. The trend can be visualized through a graph, where the thickness can be plotted on the x-axis and the PCE on the y-axis. The resulting curve would show a peak at 40 nm, as shown in figure 5a and a decline towards lower and higher thickness values. Overall, the data suggest that the thickness of the material is an important factor in determining its PCE, and an optimal thickness exists where the efficiency is maximum.

PCBM Thickness

This study investigates the impact of varying PCBM thickness on Al_2O_3 ETL on performance metrics—FF, J_{sc}, and V_{oc}. PCBM thickness ranged from 20 nm to 100 nm, while the Al_2O_3 layer was held constant at 30 nm. Maintaining a diffusion length more significant than the cell thickness is crucial for observing fluctuations between device parameters and ETL thickness. The study also reveals a significant proportionality between FF, V_{oc}, and thickness, suggesting that ETL thickness influences performance. Increased recombination rates of free charge carriers within the ETL directly impact the photoactive layer, affecting device performance (Mandadapu, 2017). As ETL thickness increases, more photon absorption occurs, but so does the recombination rate (Deepthi *et al*., 2021). The decrease in FF for PCBM ETL thickness might be attributed to increased series resistance (Bag *et al*., 2020), as photon absorption generates excitons unable to traverse the depletion layer. Elevated charge carrier recombination rates result in a more significant reverse saturation current, decreasing V_{oc} (Mandadapu, 2017).

Additionally, heightened exciton generation leads to improved PCE and Jsc, impacting overall performance (illustrated in Figure 5 concerning PCE and PCBM ETL thickness). However, excessive thickness increases resistance, more defects, and higher recombination rates, diminishing crucial values such as PSC efficiency (Tan *et al.*, 2016). Moderation in thickness, particularly at 40 nm, allows efficient transmission of photon energy to the perovskite layer, generating numerous excitons and enhancing efficiency. Hence, higher layer thickness could potentially increase diffusion length and recombination rates, thereby reducing PCE. Based on simulation analysis, the combined PCBM/Al_2O_3 ETL thickness ideal for performance was 70 nm.

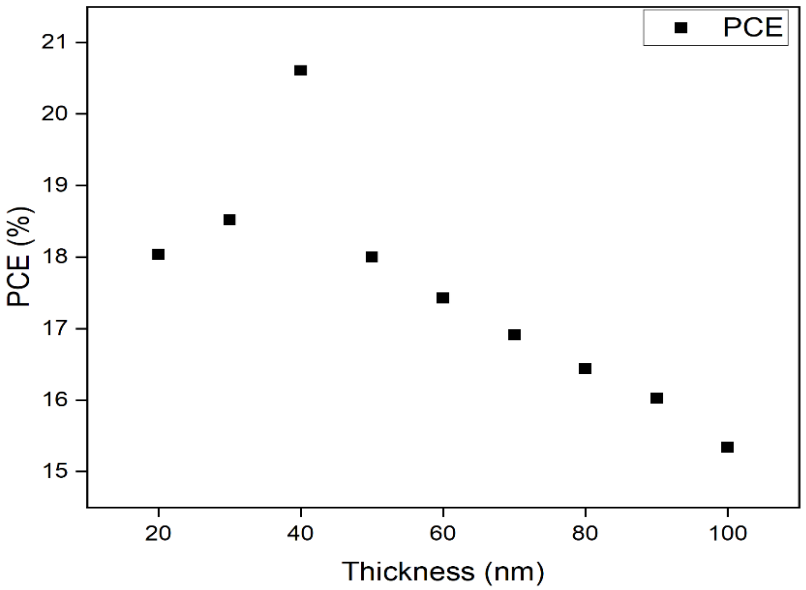

Figure 5: The thickness vs PCE graph of the simulated PCBM on Al_2O_3

Fill Factor (FF)

Table 3 presents the PCBM thickness deposited on the Al_2O_3 ETL layer in a PSC and the FF percentage derived through simulation using SCAPS 1D software. The study optimized PSC performance by varying PCBM thickness on the Al_2O_3 ETL, analyzing resulting FF percentages via simulation software. FF reflects the solar cell's efficiency in converting sunlight into electrical power—a crucial parameter impacting PSCs' PCE. It is intricately tied to interfacial charge transfer processes, showcasing its significance in PSCs. Our demonstration revealed decreased FF factors as ETL thickness increased, as depicted in Figure 6. The direct relationship between FF and the device's PCE underscores the importance of a moderate thickness when fabricating PSC devices. Therefore, optimizing PSC performance necessitates a balanced approach to ETL thickness to enhance FF, ultimately contributing to improved PCE.

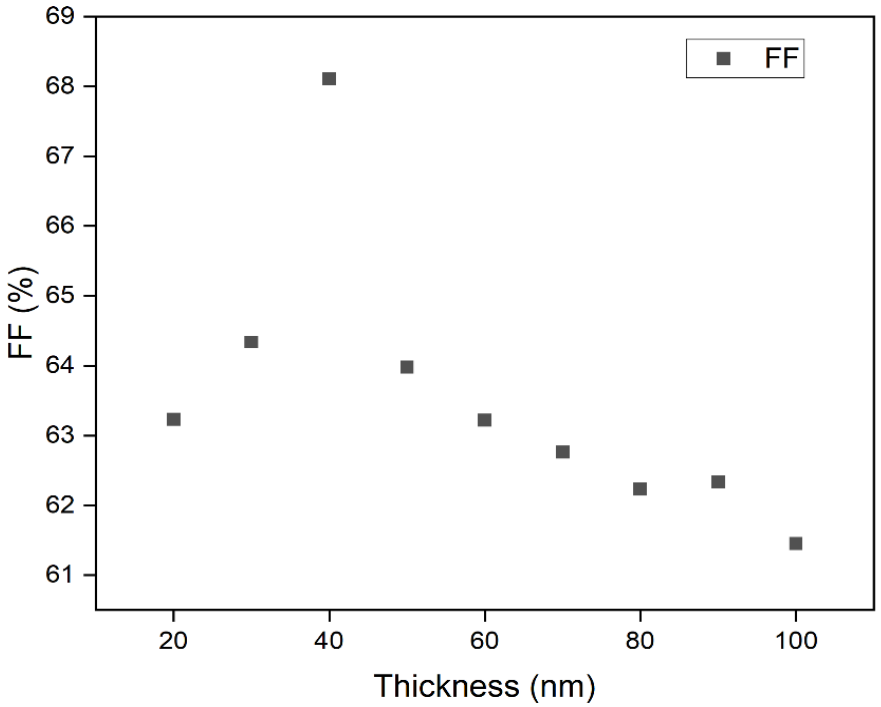

Figure 6: The graph of FF vs thickness of the PCBM ETL on Al_2O_3 ETL

Table 3: Various FF and thicknesses of the simulated PCS PCBM on Al_2O_3 ELT

Thickness (nm)	FF (%)	PCE (%)
Al_2O_3 (30 nm)	61.39	10.87
20	63.23	18.04
30	64.34	18.52
40	68.11	20.61
50	63.98	18.00
60	63.22	17.43
70	62.76	16.91
80	62.23	16.44
90	62.34	16.03
100	61.45	15.34

The table depicts a notable trend in FF percentage concerning varying PCBM thickness on the Al_2O_3 ETL, ranging from 20 to 100 nm. As thickness increases, FF rises significantly from 61.45% to 68.11%. However, deviations occur with thicknesses above 50 and below 40 nm, decreasing FF percentage. Notably, a distinct decline is evident at an 80 nm thickness, dropping to 62.23%. This observation points to an optimal thickness range for PCBM on the Al_2O_3 ETL, approximately around 40 nm, showcasing the highest FF percentage. This optimal range might vary based on other factors, including ETL material type, fabrication methods, and specific experimental conditions. These factors influence the ideal thickness range, warranting consideration in PSC design and optimization.

Temperature on Device Performance

Temperature significantly impacts the performance of a PSC. While the device's testing temperature is maintained at 300 K, operating conditions often exceed this (Raga & Fabregat-Santiago, 2013). In the simulated model, the temperature range was explored from 200 K to 500 K to understand how temperature affects the electrical performance of a solar cell, particularly after achieving optimized simulated efficiency. Figure 7 illustrates the temperature-induced changes in the PCE. Notably, the simulated device's efficiency declines as temperature rises. At 500 K, the efficiency reaches 4.96%, indicating a decrease from the optimized efficiency level. This observation emphasizes the sensitivity of PSCs to temperature variations, where elevated temperatures can adversely affect their electrical performance and overall efficiency.

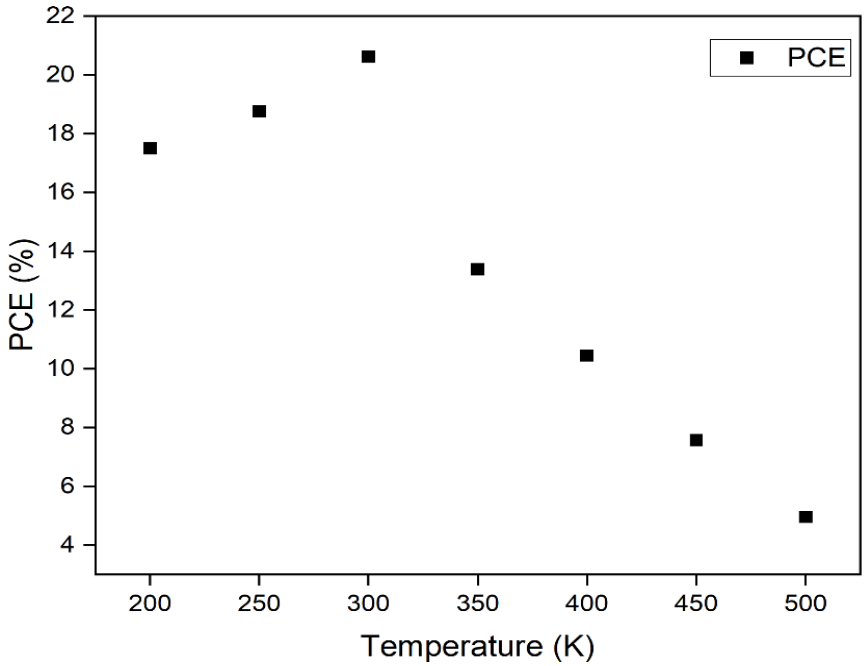

Figure 7: The graph of the optimised PSC device efficiencies against temperatures.

Table 4: Various FF, V_{oc}, J_{sc}, and PCE of the simulated PCS temperatures

Temperature (K)	V (V)	J_{sc} (mA/cm^2)	FF (%)	PCE (%)
200	3.9123	24.1927	19.55	17.50
250	1.7636	24.1901	41.66	18.77
300	0.9332	35.5830	83.45	20.61
350	0.7525	24.1754	73.54	13.38
400	0.6284	24.1688	68.80	10.45
450	0.5033	24.2075	62.17	7.57
500	0.3788	24.2592	54.00	4.96

The influence of temperature on the structural integrity of layers due to deformation and heightened stress can lead to increased interconnection among layers. This, in turn, may elevate series resistance, subsequently reducing FF and PCE as diffusion length decreases (Slami & Belkaid, 2020b). In the provided table 4 detailing temperature (K) and corresponding PCE (%) of PSCs with PCBM deposited on Al_2O_3 ETL, optimized using SCAPS 1D simulation software, noteworthy observations emerge. The highest PCE of 20.61% is evident at 300 K, signifying optimal performance at this temperature. However, both lower and higher temperature values exhibit a decline in PCE. Specifically, at higher temperatures, there is a sharp drop in PCE, plummeting to 4.57% at 500 K. Figure 7 visualizes this trend, indicating a peak at 300 K with a subsequent decline towards lower and higher temperatures. Collectively, this dataset underscores the critical role of temperature in determining PCE in PSCs with Al_2O_3/PCBM ETL optimized through SCAPS 1D simulation software. The optimal temperature for achieving the highest PCE is 300 K, with substantial reductions observed at lower and higher temperature values. This emphasizes the significance of temperature control and optimization in maintaining or enhancing PSC performance.

CONCLUSION

Choosing ETLs like PCBM and Al_2O_3 in PSCs is pivotal, considering their critical role in device performance. The Al_2O_3/PCBM layer combination enhances electron extraction efficiency, reduces charge recombination losses, and bolsters overall device stability. PCBM's effectiveness as an electron acceptor and excellent electron transport properties complement Al_2O_3's high electron affinity. Together, they form a robust interface between the perovskite layer and the electrode, curbing ion diffusion and minimizing interface defects. Implementing an Al_2O_3/PCBM ETL remarkably enhances PSCs' PCE, stability, and reproducibility. Optimization efforts using SCAPS-1D focused on fine-tuning PCBM on Al_2O_3 ETL thickness and establishing its correlation with FF. Employing the FTO/Al_2O_3/PCBM/$CH_3NH_3PbI_3$/Spiro-OMeTAD/Ag architecture for varied thicknesses, the simulation studied FF variations concerning different thicknesses and temperature impacts on the device. Results showcased that PSC optimization with PCBM thicknesses of 20 nm and 100 nm led to a maximum PCE of 10.87% for PCBM-only ETL and an optimized PCE of 20.6% for PCBM/Al_2O_3 ETL at a temperature of 300 K. Additionally, a deduced inverse relationship between FF and PSC thickness was observed. These findings emphasize that optimizing Al_2O_3/PCBM ETL significantly enhances the PCE of photovoltaic devices, underscoring its potential in advancing solar cell technology.

REFERENCES

Azri, F., Meftah, A., Sengouga, N., & Meftah, A. (2019). Electron and hole transport layers optimization by numerical simulation of a perovskite solar cell. *Solar Energy*, *181*, 372–378. https://doi.org/10.1016/j.solener.2019.02.017

Bag, A., Radhakrishnan, R., Nekovei, R., & Jeyakumar, R. (2020). Effect of absorber layer, hole transport layer thicknesses, and its doping density on the performance of perovskite solar cells by device simulation. *Solar Energy*, *196*, 177–182. https://doi.org/10.1016/j.solener.2019.12.014

Bouhjar, F., Derbali, L., & Marí, B. (2020). High performance novel flexible perovskite solar cell based on a low-cost-processed ZnO:Co electron transport layer. *Nano Research*, *13*(9), 2546–2555. https://doi.org/10.1007/s12274-020-2896-4

Brown, T. M., de Rossi, F., di Giacomo, F., Mincuzzi, G., Zardetto, V., Reale, A., & Carlo, A. di. (2021). *Progress in flexible dye solar cell materials, processes and devices*.

Burgelman, M., Decock, K., Niemegeers, A., Verschraegen, J., & Degrave, S. (2021). *SCAPS manual*.

Danladi, E., Gyuk, P. M., Tasie, N. N., Egbugha, A. C., Behera, D., Hossain, I., Bagudo, I. M., Madugu, M. L., & Ikyumbur, J. T. (2023). Impact of hole transport material on perovskite solar cells with different metal electrode: A SCAPS-1D simulation insight. *Heliyon*, *9*(6). https://doi.org/10.1016/j.heliyon.2023.e16838

Danladi, E., Kashif, M., Ichoja, A., & Ayiya, B. B. (2023). Modeling of a Sn-Based HTM-Free Perovskite Solar Cell Using a One-Dimensional Solar Cell Capacitance Simulator Tool. *Transactions of Tianjin University*, *29*(1), 62–72. https://doi.org/10.1007/s12209-022-00343-w

Deepthi Jayan, K., & Sebastian, V. (2021). Comprehensive device modelling and performance analysis of $MASnI_3$ based perovskite solar cells with diverse ETM, HTM and back metal contacts. *Solar Energy*, *217*, 40–48. https://doi.org/10.1016/j.solener.2021.01.058

Erazo, E. A., Gómez, M., Rios, L., Patiño, E. J., Cortés, M. T., & Ortiz, P. (2021). Electrodeposited PEDOT: PSS-Al_2O_3 improves the steady-state efficiency of inverted perovskite solar cells. *Polymers*, *13*(23). https://doi.org/10.3390/polym13234162

Goje, A. A., Ludin, N. A., Teridi, M. A. M., Syafiq, U., Ibrahim, M. A., Nawab, F., & Syakirin, A. A. (2023). Design and Simulation of Lead-free Flexible Perovskite Solar cell Using SCAPS-1D. *IOP Conference Series: Materials Science and Engineering*, *1278*(1), 12004.

Haidari, G. (2019). Comparative 1D optoelectrical simulation of the perovskite solar cell. *AIP Advances*, *9*(8). https://doi.org/10.1063/1.5110495

Katubi, K. M., Shiong, N. S., Pakhuruddin, M. Z., Alkhalayfeh, M. A., Abubaker, S. A., & Al-Soeidat, M. R. (2023). Over 35% efficiency of three absorber layers of perovskite solar cells using SCAPS 1-D. *Optik*, 171579.

Khalid Hossain, M., Humaun, M., Rubel, K., Toki, G. F. I., Alam, I., Rahman, F., & Bencherif, H. (2021). Effect of various electron and hole transport layers on the performance of $CsPbI_3$-based perovskite solar cells*: A numerical investigation in DFT, SCAPS-1D, and wxAMPS frameworks*.

Kuang, Y., Zardetto, V., van Gils, R., Karwal, S., Koushik, D., Verheijen, M. A., Black, L. E., Weijtens, C., Veenstra, S., Andriessen, R., Kessels, W. M. M., & Creatore, M. (2018). Low-Temperature Plasma-Assisted Atomic-Layer-Deposited SnO_2 as an Electron Transport Layer in Planar Perovskite Solar Cells. *ACS Applied Materials and Interfaces*, *10*(36), 30367–30378. https://doi.org/10.1021/acsami.8b09515

Lee, M., Choi, E., Soufiani, A. M., Lim, J., Kim, M., Chen, D., Green, M. A., Seidel, J., Lim, S., Kim, J., Dai, X., Lee-Chin, R., Zheng, B., Hameiri, Z., Park, J., Hao, X., & Yun, J. S. (2021). Enhanced Hole-Carrier Selectivity in Wide Bandgap Halide Perovskite Photovoltaic Devices for Indoor Internet of Things Applications. *Advanced Functional Materials*, *31*(16). https://doi.org/10.1002/adfm.202008908

Lin, L., Jiang, L., Qiu, Y., & Yu, Y. (2017). Modeling and analysis of HTM-free perovskite solar cells based on ZnO electron transport layer. *Superlattices and Microstructures*, *104*, 167–177. https://doi.org/10.1016/j.spmi.2017.02.028

Mandadapu, U. (2017). Simulation and Analysis of Lead based Perovskite Solar Cell using SCAPS-1D. *Indian Journal of Science and Technology*, *10*(1), 1–8. https://doi.org/10.17485/ijst/2017/v11i10/110721

Mandadapu, U., Vedanayakam, S. V., & Thyagarajan, K. (2022.). *Numerical Simulation of Ch 3 Nh 3 PbI 3-X Cl x Perovskite solar cell using SCAPS-1D*. www.ijesi.org

Raga, S. R., & Fabregat-Santiago, F. (2013). Temperature effects in dye-sensitized solar cells. *Physical Chemistry Chemical Physics*, *15*(7), 2328–2336. https://doi.org/10.1039/c2cp43220j

Reyes, A. C. P., Lázaro, R. C. A., Leyva, K. M., López, J. A. L., Méndez, J. F., Jiménez, A. H. H., Zurita, A. L. M., Carrillo, F. S., & Durán, E. O. (2021). Study of a lead-free perovskite solar cell using CZTS as HTL to achieve a 20% PCE by SCAPS-1D simulation. *Micromachines*, *12*(12). https://doi.org/10.3390/mi12121508

Slami, A., & Belkaid, A. B. (2020 a). *Numerical Study of Based Perovskite Solar Cells by SCAPS-1D Solar cells View project Solar cells View project*. https://www.researchgate.net/publication/337797426

Slami, A., & Belkaid, A. B. (2020 b). *Numerical Study of Based Perovskite Solar Cells by SCAPS-1D Solar cells View project Solar cells View project*. https://www.researchgate.net/publication/337797426

Slami, A., & Merad, L. (2022). *Numerical Study of Based Perovskite Solar Cells by SCAPS-1D*.

Tan, K., Lin, P., Wang, G., Liu, Y., Xu, Z., & Lin, Y. (2016 a). Controllable design of solid-state perovskite solar cells by SCAPS device simulation. *Solid-State Electronics*, *126*, 75–80. https://doi.org/10.1016/j.sse.2016.09.012

Tan, K., Lin, P., Wang, G., Liu, Y., Xu, Z., & Lin, Y. (2016 b). Controllable design of solid-state perovskite

solar cells by SCAPS device simulation. *Solid-State Electronics*, *126*, 75–80. https://doi.org/10.1016/j.sse.2016.09.012

Wang, K. L., Zhou, Y. H., Lou, Y. H., & Wang, Z. K. (2021). Perovskite indoor photovoltaics: opportunity and challenges. In *Chemical Science* (Vol. 12, Issue 36, pp. 11936–11954). Royal Society of Chemistry. https://doi.org/10.1039/d1sc03251h

Yang, D., Zhang, X., Wang, K., Wu, C., Yang, R., Hou, Y., Jiang, Y., Liu, S., & Priya, S. (2019). Stable Efficiency Exceeding 20.6% for Inverted Perovskite Solar Cells through Polymer-Optimized PCBM Electron-Transport Layers. *Nano Letters*, *19*(5), 3313–3320. https://doi.org/10.1021/acs.nanolett.9b00936